Paper II

Yongjia Song, Nils Gunnar Kvamstø, Pascal Mailier, David B. Stephenson (2007)

Properties of latitudinally directed cyclone tracks in NCEP data and in the ARPEGE general circulation model.

Properties of latitudinally directed cyclone tracks in NCEP data and in the ARPEGE general circulation model

Yongjia Song[1*], Nils Gunnar Kvamstø[1,2], Pascal Mailier[3] , David B. Stephenson[3,2]

[1]Bjerknes Centre for Climate Reasearch, University of Bergen, Norway.
[2]Geophysical Institute, University of Bergen, Norway.
[3]Department of Meteorology, University of Reading, UK.

Abstract

Cyclone tracks that occurred in the Northern Hemisphere during 47 extended winters (1950/1 - 1997/11) has been identified from NCEP reanalyses by means of an objective tracking method (Hodges 1995, 1996). The tracks have been divided into two classes, one with northward moving cyclones and a second with southward moving cyclones. The criteria for this selection are that a cyclone track crosses any longitude section from either side (south or north). In both cases mean number of occurrence, variance and seriality (succession of cyclone occurrence) at a grid point level have been investigated. Corresponding cyclone track datasets have been derived from a simulation with the atmospheric model ARPEGE, forced with observed monthly SSTs from 1950 – 1997. The diagnostics listed above have been computed from the model data sets and compared with those based on observations (reanalyses). The winter mean distribution of northward moving cyclone transits in NCEP reanalyses resembles the corresponding distribution of eastward cyclone transits shown in recent literature. This is also the case for variability of monthly counts during winter. Both of the winter mean distributions have a high degree of similarity to other measures of storm track activity. Northward moving cyclones in ARPEGE appears similarly, both with respect to mean distribution and variance, but with a substantial difference that the number of occurrences is 30% lower in the model data as compared with NCEP data. The three regions where we find high numbers of southward moving cyclones correspond well in the two datasets, again with the model data containing 35% less cyclone counts than the NCEP data. A dispersion coefficient has been computed showing that for northward moving cyclones in the Pacific and Atlantic storm tracks, regularity is found in the westernmost parts while clustering occurs in central (Pacific) and eastern (North Atlantic) parts. The spatial distribution and degree of clustering and regularity is in overall agreement between the model- and NCEP data. The three regions with significant NS occurrences are associated with clustering in both datasets. The link between the monthly cyclone counts and the large-scale circulation, represented by the ten leading rotated principal components of monthly geopotential at 750hPa, was investigated. It was found that the NAO does not have as dominating influence in determining the cyclone count variability as could be expected on basis of earlier literature. Namely, four additional patterns are actively affecting cyclone occurrences in various regions in the North Atlantic and European sector. For NCEP data we found similar behaviour between northward cyclone transits and eastward moving cyclones in this respect. The link between monthly cyclone counts and large scale flow is very different in NCEP data than in the model data.

1. Introduction

In Mailier et al. (2006) (hereafter denoted as M06) it is pointed out that serial storms are one of three cyclone classes that can have devastating effects on European economy. Serial storms cluster in time and occur typically when successive unstable waves develop and move rapidly along the trailing front in wake of a large "parent" low. M06 developed a statistical framework to study seriality of storms. This framework was applied on 48,818 cyclone tracks which occurred during 53 extended winters (October-March 1950/1-2003/3). The tracks were calculated by identifying and connecting maxima in 6 hourly relative vorticity fields at 850hPa (ξ_{850}) during the period. In establishing the statistical framework, M06 demonstrated that the succession of cyclone occurrence at a location can be considered as a point process. They further showed that the Poisson process is convenient to use for statistical modelling of occasional time aggregation of extra-tropical cyclones. By analysing the rate of the Poisson process and quantifying how it affects the mean number and the variance of cyclone occurrences during a given time interval, M06 derived a coefficient of dispersion that determines the degree of clustering (or regularity) of cyclone occurrences. In addition they used Poisson regression to explore any linkage between storm seriality and large-scale flow. An occurrence is defined as a transit of a low pressure (or cyclone) trajectory across a $10\,^{\circ}$ latitudinal section through any grid-point. All cyclone tracks subject to analysis in M06 have a starting point west of the end point.

By examining the spatial distribution of the dispersion coefficient, M06 found more serial clustering than expected due to chance (overdispersion) in the exit of the North Atlantic storm tracks, tracks over Europe and central North Pacific. The clustering was found to be associated with cyclones of higher intensity ($\xi_{850} \geq 0.5 f$). On the other hand, undersdispersion, or higher regularity than expected due to chance, was found in the entrance of the North Pacific and North Atlantic storm tracks. M06 attributes this fact to the permanent baroclinic forcing that prevails in these regions. The results of their Poisson regression showed that the variation of monthly cyclone occurrences over Europe is largely accounted for by modes of climate variability with lower frequency than the synoptic scale. The five patterns found to be important are: The North-Atlantic Oscillation (NAO), the East-Atlantic pattern (EAP), the East Atlantic/West Russian pattern and the Polar/Eurasian pattern. M06 emphasizes that the NAO alone is not sufficient to account for the variability of cyclone rates in the North Atlantic and western Europe.

M06 based their analysis on cyclone trajectories that crossed meridional transects. The cyclone tracks subjected to analysis had only the criterion that the end point should be east of the starting point. Many cyclone tracks have a cross latitudinal component particularly in the eastern part of the ocean basins. One of the purposes with this work is to investigate how serial properties depend on the cross latitudinal orientation. Hence we

will explore cyclone tracks where the end point is either north or south of the starting point. Tracks that are parallel to latitude transects will not be included in this analysis. In the storm track exit regions it is assumed that few cyclone tracks have no cross latitudinal component. Also if we assume that a negligible part of the cyclone tracks crossing latitudinal transects have an easterly component, such an analysis will be complementary to M06 since the dataset of cyclone tracks subjected to analysis to a large extent will be the same in the two cases.

It is a well known fact that most General Circulation Models (GCM) have a storm track climatology which shows a too zonal North Atlantic storm track in the exit region (Doblas-Reyes at al. 1998; Lopez et al. 2000). It is thus of particular scientific interest to obtain a description and understanding of the seriality of cross latitudinal cyclone tracks in both observations and in GCM data. A second scientific issue of this work is to explore seriality of meridionally directed cyclone tracks in a GCM and how it compares with observationally based data.

The paper is arranged as follows. In section 2 we present the data, model and methods. Results from analysis of observationally based cyclone tracks are listed in section 3 while corresponding results for GCM cyclone tracks are presented in section 4. A summary and conclusions are presented in section 5.

2. Data, model and methods

2.1 Data

In order to compute cyclone tracks, we have used 6-hourly reanalyses during 53 extended winters, October to March 1950/51-2002/3, from the National Centers for Environmental Prediction - National Center for Atmospheric Research (NCEP/NCAR) (Kalnay et al. 1996). These data have been freely downloaded from the NOAA-CIRES Climate Data Center, Boulder, Colorado, USA (http://www.cdc.noaa.gov/). As pointed out in M06, extended winters (ONDJFM) are preferred to the more conventional DJF season in order to avoid missing cyclones that occur in autumn and spring.

Zonal and meridional wind components at 850hPa in the Northern Hemisphere were used to compute ξ_{850}. An advantage with ξ_{850} is that this field has little influence from the background state hand highlight thus small scale features. Also cyclones can be earlier detected using ξ_{850} instead of the sea level pressure.

There is little difference between lower tropospheric cyclone track statistics based on NCEP/NCAR reanalyses and reanalyses from the European Centre for Medium-range Weather Forecasts (ECMWF) ERA-15 (Hodges et al. 2003).

2.2 Cyclone track algorithm

The ξ_{850} field can be very noisy with frontal systems beginning to be resolved, the processing is therefore performed at a spectral resolution of T42. The reduction in resolution associated with the T42 truncation provides some smoothing of the higher frequencies. In addition planetary scales for total wave numbers $n \leq 7$ are removed from the field using a filtering method discussed by Anderson et al. (2003). This spectral cut off does not make any significant change to the results since the planetary scales are relatively weak in the vorticity fields relative to the anomalies. The retained fields are searched for local extremes, which are the centres for negative and positive vorticity anomalies. In this study we have concentrated on the positive vorticity anomalies (cyclones), the feature points associated with low-pressure systems. The feature points for two consecutive time steps are linked together using a nearest neighbour search. A cost-function based on track smoothness in terms of changes in direction and speed (Hodges, 1995, 1996) is calculated for each possible ensemble of trajectories. The ensemble minimizing the cost-function is chosen to be the best fit and thereby restricts the feature to physical movement. The technique has been generalized to the spherical domain (Hodges, 1995), which obviates the need to use projections, which may introduce systematic biases (Zolina and Gulev, 2002). This allows the analysis of global data or large spherical regions to be performed. Semi-stationary storms (less than 10 º total displacement) and short-lived storms (lifetime less than 2 days) are removed.

We here focus our attention on the cyclone track occurrence itself, but calculation of descriptive statistics is provided by the use of spherical nonparametric estimators from the ensembles of feature tracks (Hodges, 1996). Here, we will only use intensity, which is computed from the size of the anomalies in relative vorticity for the feature points; unit is 10^{-5} s^{-1}.

2.3 The ARPEGE GCM

The atmospheric GCM used in this study is version 3 of the ARPEGE/IFS model used operationally by Météo-France and developed jointly by Météo-France and ECMWF (Déqué et al. 1994, 1998; Doblas-Reyes et al. 1998). In the version used here, we use a radiation scheme by Morcrette (1991), convective wave drag parametrisation by Bossouet et al. (1998), snow scheme by Douville et al. (1995) and increase of orographic wave drag by Lott and Miller (1995). In our experiments we employ semi-Lagrangian time intergration and a so-called linear truncation (Hortal 1998) at wave number 63 ($T63_L$) in the horizontal. This corresponds to a latitude-by-longitude grid spacing of approximately 2.8 ° by 2.8 °. The vertical discretization (Simmons and Burridge 1981) consists of 31 layers of which 20 are in the troposphere.

In order to explore the representation of cyclone tracks in ARPEGE, we have generated a simulation where observationally based monthly global sea surface temperature (SST) fields from 1950 – 1997 are employed as lower boundary condition. The SST dataset is

constructed from two GISST (Global Sea Ice and Sea Surface Temperature) datasets (Reynolds and Smith, 1994), namely the GISST 2.3 from 1950 to 1982 and the newer GISST 3.0 from 1983 to 1997. The model was integrated from January 1950 to November 1997 with slightly different initial conditions. For the consistency, all storm track statistics, both for the observation and simulation, are taken over this period.

3. Results

3.1 Mean cyclone occurrence

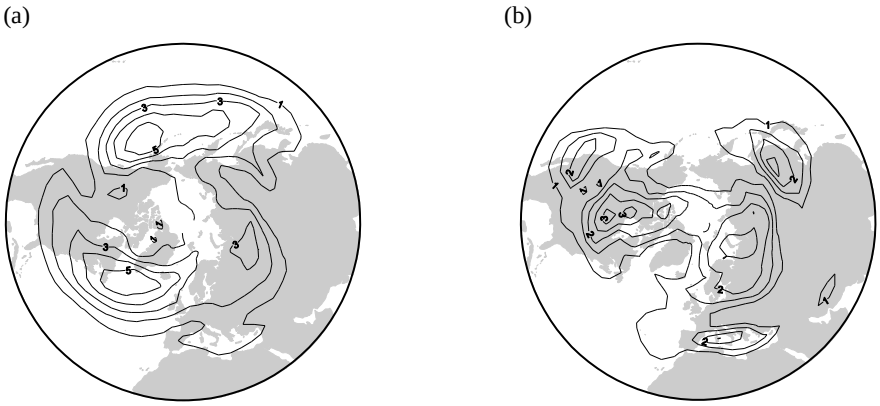

Figure 1. Sample mean $\bar{n}$ of the monthly counts of a) South-North directed cyclone transits, contours start at 1 *month*$^{-1}$, with contour intervals of 1 *month*$^{-1}$. b) North-South directed cyclone transits, contours start at 1 *month*$^{-1}$, with contour intervals of 0.5 *month*$^{-1}$. The diagnostics are based on NCEP data.

In M06 it was found that the west to east (WE) travelling cyclone counts qualitatively resembled track density maps (i.e. in Hoskins and Hodges 2002) where one of the characteristics was the maxima in the westernmost parts of the two ocean basins. In the case with south to north (SN) travelling cyclones, we find a similar gross qualitative agreement, but not to the same extent as in the WE case. In figure 1a the distribution of the 53 winter mean $\bar{n}$ of monthly cyclone transits past a longitudinal section with length equivalent to 10 ° at 50 ºN through each grid point is shown. From this figure we see that the SN transit counts ranges from 0 – 6 month^{-1} and typical values in the North Pacific and North Atlantic storm tracks generally are around 2 – 6 month^{-1}. Regions with values above 2 month^{-1} can thus be said to form the storm track regions. The highest values of SN counts in the two main storm track regions are displaced to the east compared with the WE case (M06). In the Pacific we find the SN maximum on the eastern side of the basin and the Atlantic maximum is found south of Greenland.

The pattern of winter mean number of southward moving cyclones is fundamentally different from the two others. This pattern is characterised by three maxima with peak values around 3 month^{-1}: One over central Canada and North America, a second over northern Siberia and a third over north east China. A weaker secondary maximum is

found in the Mediterranean Sea. Outside these maximum areas relatively small values are found.

It is worthwhile to note that the maxima over central Canada/North America and Siberia have large overlaps with maxima in the WE transit counts shown in M06.

3.2 Time series

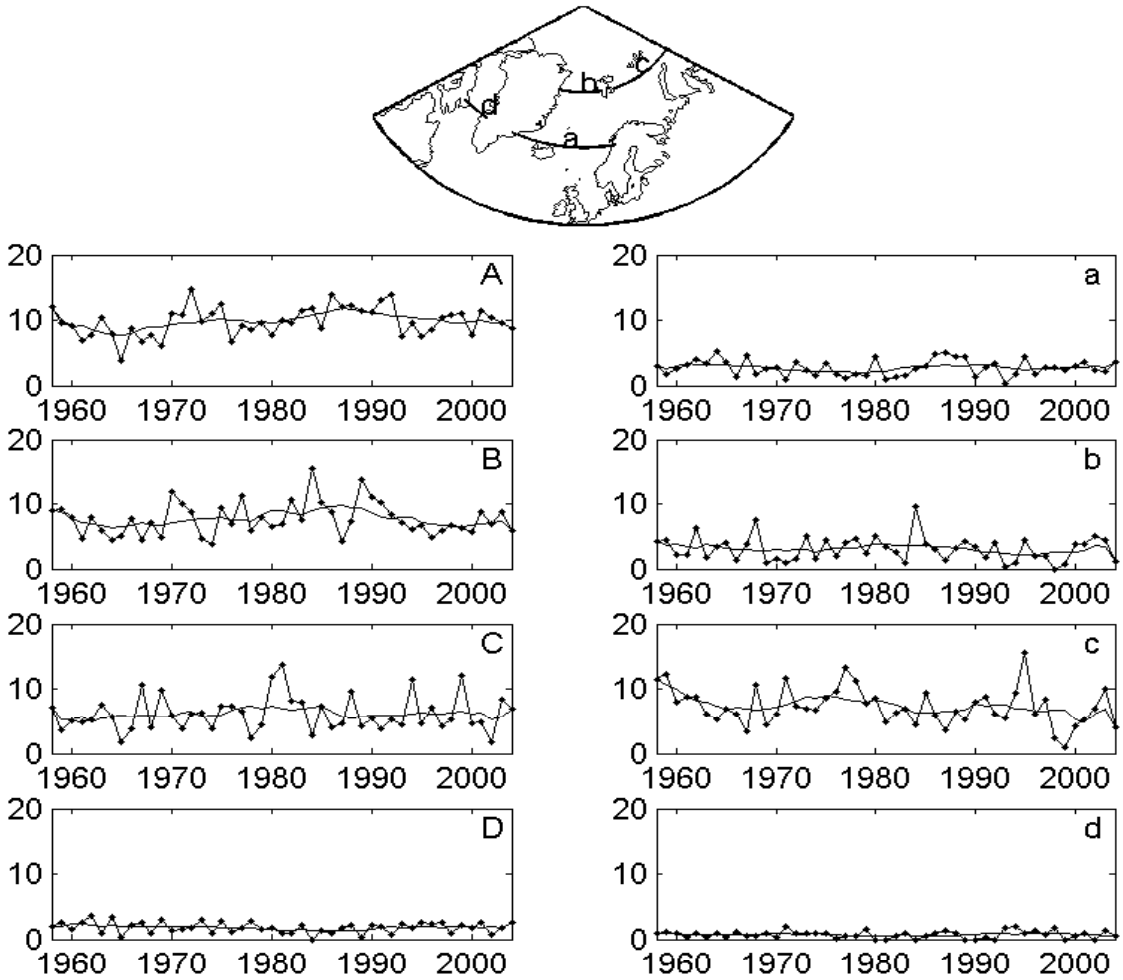

Figure 2.Time series for total number of cyclone tracks crossing four different latitudinal cross sections in the North Atlantic shown in top panel during the winters (ONDJFM) from 1958-2003. The number of cyclone tracks is displayed as the line with asterisk, another is the 11 years smooth curve. Figures 2A, B, C and D are based on counts on South-North directed tracks, while a, b, c and d are based on North-South directed tracks. The counts are based on NCEP data.

Variations of storm track counts with time can, for selected longitudinal sections, be seen in figure 2. Standard statistics for the different time series are given in table 1. From both sources it can be seen that the mean number of counts is positively correlated with the variance (s^2). This is in accordance with findings M06 for WE cyclone counts. Maps of s^2 (not shown) show also a high degree of similarity with the winter mean number of transits in many regions. Except for the Barents Sea section, we generally find a higher number of SN counts than NS counts.

(a)

	A	B	C	D
$\bar{n}$	9.8	7.6	6.1	1.8
σ	2.3	2.5	2.8	0.8
σ_{11}	1.0	1.0	0.6	0.3

(b)

	a	b	c	d
$\bar{n}$	2.7	3.1	7.3	0.7
σ	1.2	1.9	2.9	0.5
σ_{11}	0.4	0.6	1.3	0.1

Table 1. Standard statistics for the different time series. $\bar{n}$ is monthly counts of storm track, σ and σ_{11} represent standard deviation and its smoothed result with 11 years respectively. A, B, C and D are based on counts on South-North directed tracks, while a, b, c and d are based on North-South directed tracks.

3.3 Stochastic modelling of cyclone transits

The number of cyclone transit through any longitude segment can be considered as a Poisson process. M06 demonstrated that a dispersion coefficient $\hat{\psi}$, which identifies discrepancies between the 53 winter mean $\bar{n}$ of monthly totals n_i of cyclone transits and the 53 winter variance s^2 of the monthly transit counts, can be used to interpret the time behaviour of the cyclones:

$$\hat{\psi} = \frac{s_n^{\,2}}{\bar{n}} - 1 \qquad (1)$$

$\hat{\psi} \approx 0$: This is consistent with a purely random process with constant rate.

$\hat{\psi} > 0$: Indication of overdispersion in the distribution of monthly transit counts. This case is consistent with a process that is more clustered in time than a purely random process.

$\hat{\psi} < 0$: Indication of underdispersion and this case is consistent with a process that is more regular than a purely random process with constant rate.

M06 applied this statistic for interpretation of the time behaviour of WE cyclone transits and compared the storm track behaviour in the Atlantic and Pacific basins. Their main findings were that the both storm tracks exhibited underdispersion in the entrance (western side) while overdispersion was found in the exit region of the North Atlantic storm track (North Eastern side) and in the central Pacific.

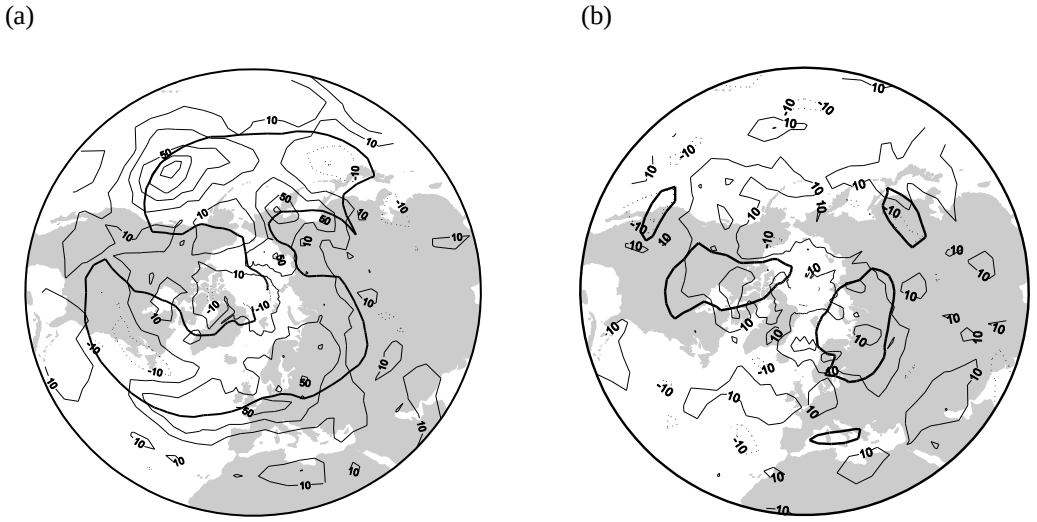

Figure 3. a) Estimated dispersion statistic $\hat{\psi}$ (in %) of the monthly number of South-North directed cyclone transits. Solid/dashed lines indicate positive/negative values. Contours start at ±10%, contour intervals at 20%. Thick grey lines represent the boundaries of the region where $\overline{n} \geq 2 month^{-1}$ (Shaded areas in Fig. 2 have been added for easy reference to the storm tracks). b) as a, but for North-South directed cyclone transits. The statistics are based on NCEP data.

Figures 3a and 3b show $\hat{\psi}$ for SN and NS transits respectively. In the SN case we find underdispersion in the westernmost part of the two ocean basins while positive values are found elsewhere with maxima over the east Pacific, east North Atlantic and Europe. In contrast, we find constant rates and/or overdispersion only in the NS case. The overdispersion maximum over the Pacific in the SN case has similar estimate values as in the WE counts (M06), while over the eastern North-Atlantic we find higher estimate values in the SN case. In other words, if we consider cyclones travelling in all directions, the SN cyclones are most strongly affected by clustering in the North Eastern Atlantic. It should also be noted that North West Siberia, which belongs to the exit region for the North Atlantic storm track, has negative values and underdispersion in the WE case while we find overdispersion only when considering SN transits.

In the case of southward moving (NS) cyclones (figure 3b), we find overdispersion only in the abundant regions and the maximum values are concentrated in two regions; over central Canada/North America and over the north-eastern Europe and Siberia (including

the Barents Sea). In both cases maximum NS dispersion values are comparable to the maximum SN values over the North Atlantic exit region.

3.4 Large scale influence

As in M06, we assume that the monthly number, *N*, of cyclone transit through any longitude segment can be considered as an inhomogeneous one-dimensional Poisson process with time-varying rate. In this case we have that

$$N \mid \mu \sim Poisson(\mu)$$

This equation must be read "N given μ is Poisson distributed with mean μ". Following M06, we can employ a logarithmic link function to relate *ln(μ)* to a linear combination of explanatory variables x_k.

$$\ln(\mu) = \beta_0 + \sum_{k=1}^{P} \beta_k x_k$$

Maximum likelihood estimates of the regression parameters β_k can be obtained by means of an iterative weighted least squares algorithm. For this study the MATLAB routine *glmfit* was used. In order to explore the large scale circulation's influence on the number of counts across latitudinally oriented transects, we have used ten teleconnection indices x_k as explanatory variables. In addition, 5 binary variables quantify the mean state of the large scale atmospheric flow for each month. Thus P=15. Ten β_k are then a measure of the individual weight of the teleconnection pattern in question.

We here use a standard rotated Empirical Orthogonal Function (EOF) analysis of monthly geopotential anomalies at 500hPa (see Appendix A).

3.4.1 Characteristic features for South-North travelling cyclones

The interpretation of the β_k - parameter can be seen as the weight (or influence) of the pattern in question on SN travelling lows' monthly transit variability. Maximum likelihood estimates of the most relevant β_k -parameters for the Atlantic European region are plotted in figure 4. High transit rates (n_i) are associated with low pressure regions in the teleconnection patterns. Areas where the individual patterns have high or significant weight (β_k) in explaining the transit rate are shaded.

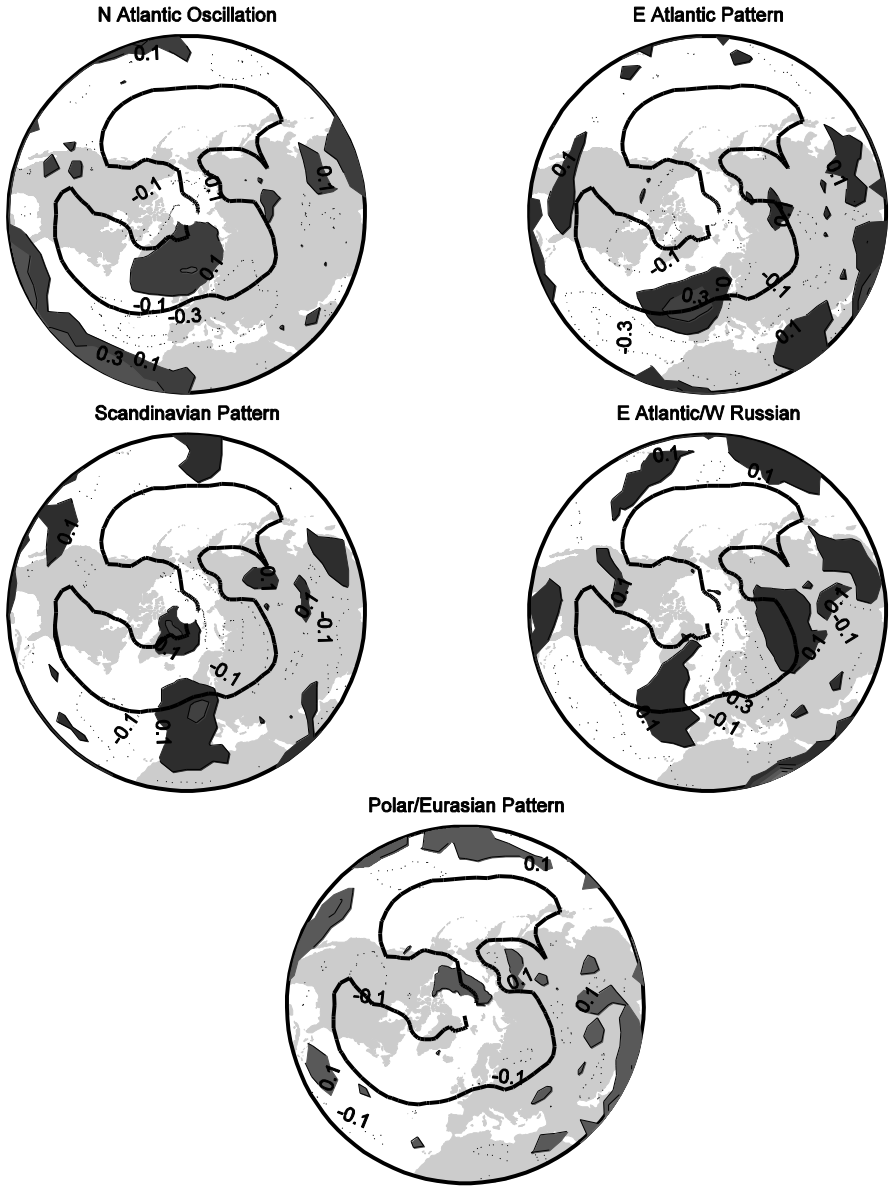

Figure 4. Estimates of the β_k parameters for the five teleconnection patterns relevant for the South-North moving cyclones in the North Atlantic and Europe. Solid/dashed lines indicate positive/negative values. Contours start at ±0.1, contour intervals of 0.2. Areas where $\beta_k \geq 0.1$ are shaded. Estimates are based on NCEP data.

The North Atlantic Oscillation (NAO) pattern has significant impact in the North Sea and Nordic Seas with the East coast of Greenland as the western boundary and Scandinavia and Novaja Zemlya as the eastern boundary of its main area of influence. In its positive phase NAO causes high transit rates in this region and low transit rates in the region from the Azores and eastward over the Mediterranean region, central European continent and into western Russia. This area is however on the outskirts of the Atlantic storm track.

The East Atlantic Pattern (EAP) has prominent influence in an area over western Europe including the British Isles. In the positive EAP phase, cyclones track south of the preferred storm track position in the eastern North Atlantic. The EAP influence on SN

cyclone counts is situated between the two opposite NAO influence regions – in other words in a region with weak NAO influence.

The influence of the Scandinavian pattern (SCP) seems also to form a dipole shape. The positive phase of the SCP causes high transit rates in central Europe and reduced rates in Siberia.

The influence of the East Atlantic/Western Russian pattern has shape similar to a wave train. During the positive phase of the East Atlantic/Western Russian pattern, we find increased SN cyclone counts in a region over the eastern North-Atlantic south of Greenland and another region over central Russia. Between these two regions, over northern and central Europe, we find reduced counts in the positive phase.

The Polar Eurasian pattern has a minor influence on the North-Atlantic cyclone tracks in the pole ward direction.

3.4.2 Characteristic features for North-South travelling cyclones

The areas where we find mean counts higher than 2 month^{-1} are encircled with thick solid contour line in figure 5. The region over central Canada and North America is mainly influenced by the NAO, which in its positive phase causes high NS cyclone transits in this region. The other region with high NS counts is situated over eastern Scandinavia, Russia, Siberia and the Barents Sea. The two patterns with influence on the NS transit variability in this region are SCP and the East Atlantic/Western Russian pattern. In the positive phase SCP causes high NS transit counts over central Siberia and Russia, while the positive phase of East Atlantic/Western Russian pattern is associated with high NS transit counts over Scandinavia, western Russia and Eastern Europe.

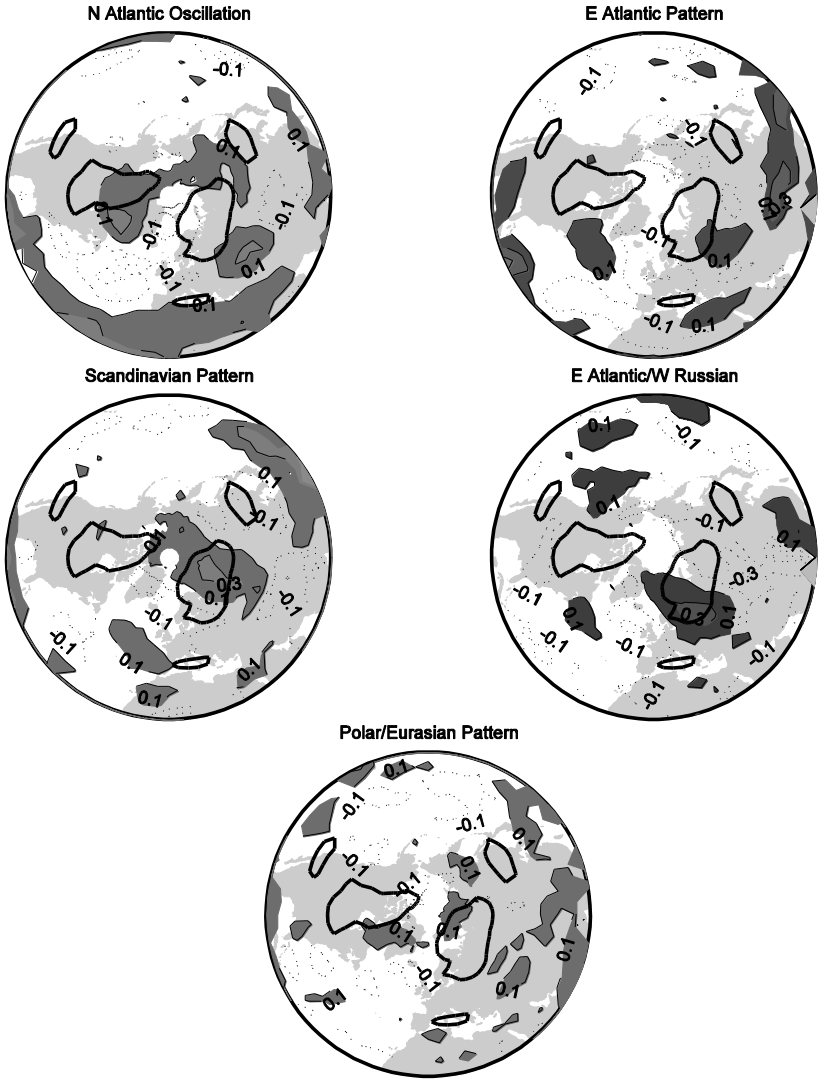

Figure 5. Estimates of the β_k parameters for the five teleconnection patterns relevant for the North-South moving cyclones in the North Atlantic and Europe. Solid/dashed lines indicate positive/negative values. Contours start at ±0.1, contour intervals of 0.2. Areas where $\beta_k \geq 0.1$ are shaded. Estimates are based on NCEP data.

4 Representation of storm-tracks in ARPEGE

4.1 Climatology

The distribution of simulated cyclone counts, in the SN and NS cases, have a very similar distribution as the observed (or NCEP) ones (figure 6). The most apparent difference between the two datasets is the overall reduction of cyclones in the model dataset. Based on the time series described in figures 2 and 7 and tables 1 and 2 (sections A-C), we find

that the winter mean number of SN (NS) cyclone counts in the model is 34% (43%) smaller than in the NCEP data.

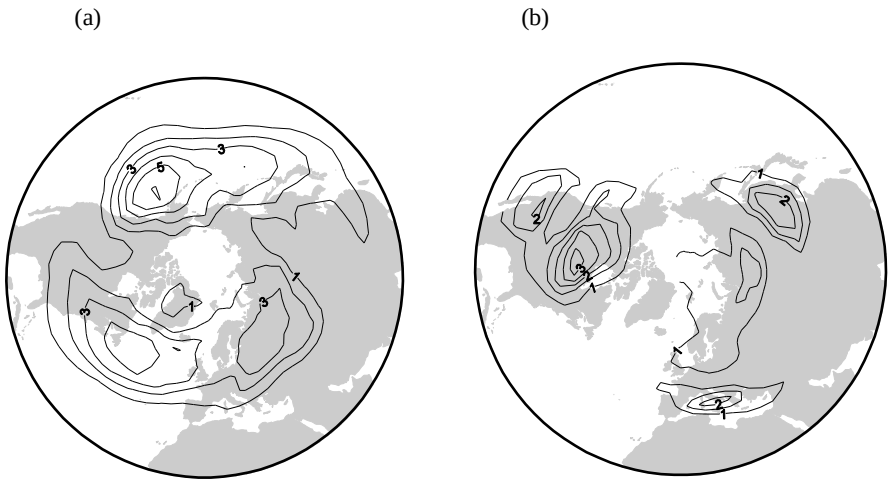

Figure 6. As Figure 1, but based on data simulated with the ARPEGE model.

(a)

	a	b	c	d
$\bar{n}$	6.3	3.9	5.0	1.4
σ	2.3	2.1	2.1	0.8
σ_{11}	0.5	0.8	1.1	0.2

(b)

	a	b	c	d
$\bar{n}$	1.3	1.7	3.9	0.7
σ	0.8	0.8	1.8	0.7
σ_{11}	0.3	0.2	0.6	0.3

Table 2. As Table 1, but based on data simulated with the ARPEGE model.

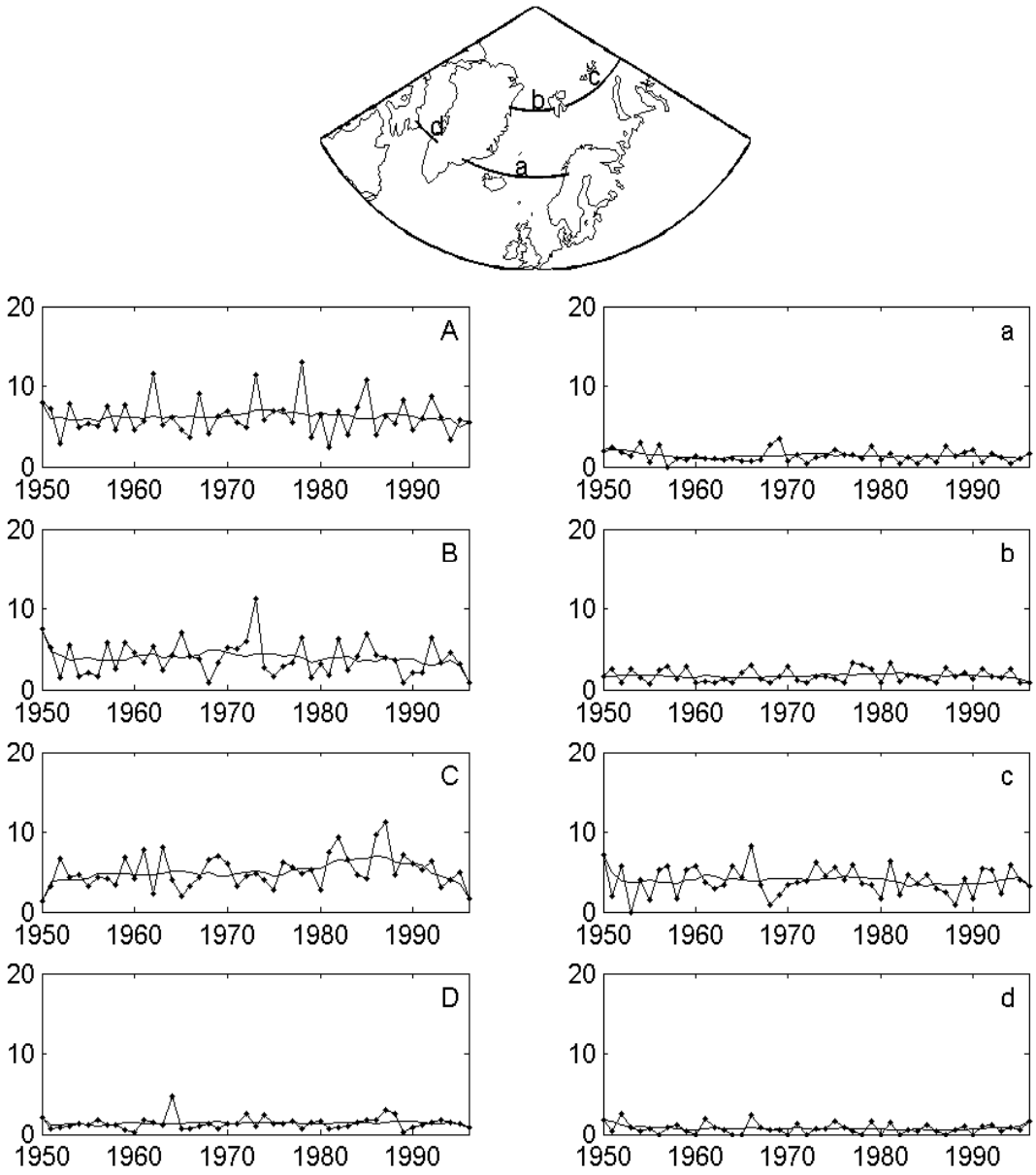

Figure 7. As Figure 2, but based on data simulated with the ARPEGE model.

4.2 Variability

There is also a corresponding decrease in variability of cyclone counts in both cyclone classes. From figure 2 and 7, we clearly see reduced amplitudes on the variations around the mean in the model data. On monthly basis the standard deviation in the model is 10% (18%) smaller than in NCEP for SN (NS) cyclones. For the longer timescales (11-year running mean) model standard deviations are 19% (18%) smaller than the corresponding

NCEP values. Numbers are based on sections A-C in table 1 and 2 (averages are weighted with the length of the sections).

4.3 Clustering and regularity

The dispersion coefficient $\hat{\psi}$ of the simulated monthly cyclone transits is shown in figures 8a and 8b. The overall distribution of simulated $\hat{\psi}$ shows similarity to the NCEP based results, both for the SN and NS cyclone transits. We find simulated overdispersion (or clustering tendency) in the central Pacific and the eastern North Atlantic, while in the westernmost parts of the two storm tracks we find underdispersion or a tendency to more regular cyclone transits. The most prominent differences when comparing observed with simulated cyclone dispersion statistics are the two overdispersion maxima situated over the Aleutians and over south eastern Greenland in ARPEGE. We also observe that the overdispersion in the central Pacific and eastern North Pacific and Europe is slightly stronger in the model.

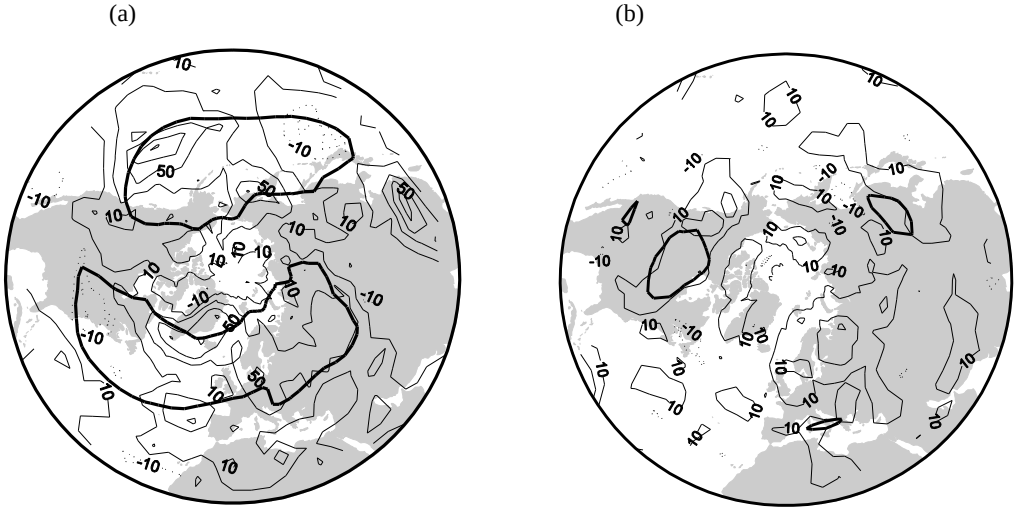

Figure 8. As Figure 4, but based on data simulated with the ARPEGE model.

4.4 Stochastic modelling

It has also been attempted to link the variability of cyclone transits across longitudinal sections through each grid point with the PCs of the leading rotated EOFs of monthly geopotential anomalies at 500hPa in the simulation. This has been done by means of Poisson regression as described in section 3.4. The β_k parameters are presented in figures 9 and 10 for the SN and NS classes respectively. As can be seen from the figure, the patterns project on the SN cyclone transit variability in a way which shows some similarity to the corresponding projections in the NCEP data. The most obvious exceptions are the East Atlantic and Polar Eurasian patterns in the model which project

on the transit variability in a completely different manner than what we observe in the NCEP data (fig. 3). As can be seen in Appendix A, the spatial structures of East Atlantic and Polar Eurasian patterns in the model do not show any resemblance to the corresponding patterns that are based on the reanalyses. For the NS class, all of the patterns project differently on the transit variability in the model as compared with the reanalyses.

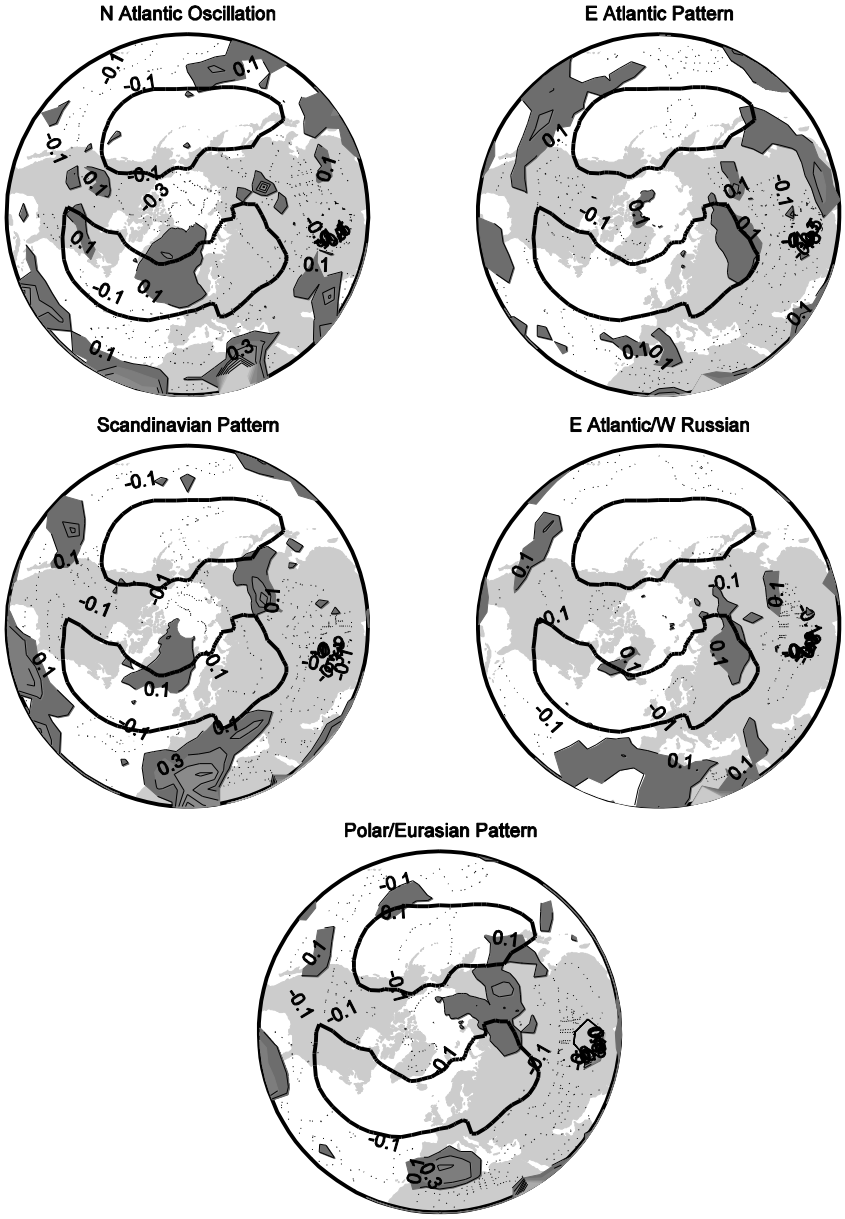

Figure 9. As Figure 5, but based on data simulated with the ARPEGE model.

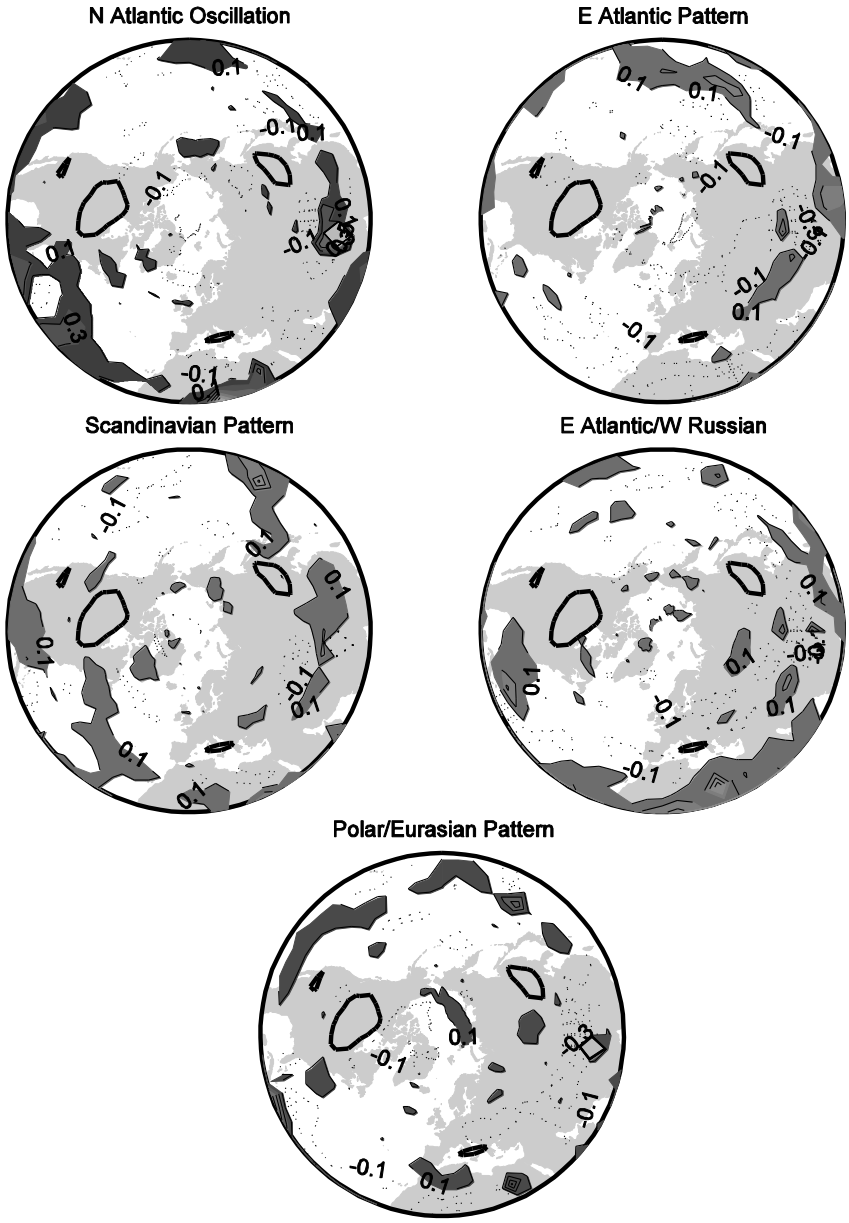

Figure 10. As Figure 6, but based on data simulated with the ARPEGE model.

5 Summary and concluding remarks

Cyclone tracks that occurred in the Northern Hemisphere during 47 extended winters (1950/1 - 1997/11) has been identified by means of an objective tracking method (Hodges 1995, 1996). The tracks have been divided in two classes, one with northward moving cyclones and a second with southward moving cyclones. The criteria for this selection are that a cyclone track crosses any longitude section from either side (south or

north). In both cases mean number of occurrence, variance and seriality (succession of cyclone occurrence) at a grid point level have been investigated.

Corresponding cyclone track datasets have been derived from a simulation with the ARPEGE model, forced with observed monthly SSTs from 1950 – 1997. The diagnostics listed above have been computed from the model dataset and compared diagnostics based on reanalyses.

To our knowledge, such an analysis of meridionally directed cyclone tracks has not been performed earlier. In the cyclone tracks investigation by M06, the only criterion for including a track in their analysis was that the end point should be east of the starting point of a trajectory. It is then certain that meridonally directed tracks are included in their analysis. However, as our study distinguishes between southward and northward moving cyclones, comparison with M06 offers the possibility to decompose structures and attribute them to either of the cyclone classes. The most characteristic features based on NCEP data can be summarized as follows:

- Spatial structures of mean cyclone counts are similar for the WE (M06) and SN moving cyclones. These patterns also resembles other measures of cyclone activity like track density (Hoskins and Hodges, 2002; Sorteberg et al. 2004) or band pass filtered variables (Blackmon 1976).
- The pattern of mean NS cyclone transits is substantially different from the two others and contains three smaller areas with significant numbers of cyclone counts.
- There is positive spatial correlation between mean number of cyclone counts and variability in all three cyclone track classes.
- As for WE (M06), we find clustering (overdispersion) of SN cyclone transits in the North Eastern Atlantic and central Pacific, while there are more regular transits (underdispersion) in the westernmost parts of the two ocean basins.
- For NS cyclone counts, we find overdispersion or constant rate (random) transits only.

The characteristics listed above can to a large extent be found in simulations with the ARPEGE GCM model as well. However, one important exception is that the number of

cyclones is systematically lower in the model data. The statistics from time series shown in figures 2 and 7 in tables 1 and 2 give that the winter mean cyclone counts in the model amounts to 69% and 64% of the counts in NCEP for the SN and NS cyclone classes, respectively. The numbers for the standard deviation of monthly counts are on average 89% and 78% for the SN and NS cyclone classes, respectively.

The link between the monthly cyclone counts and the large-scale circulation, represented by the ten leading rotated principal components of monthly geopotential at 500hPa was investigated. It was found that the NAO does not have as dominating influence in determining the cyclone count variability as could be expected on basis of earlier literature. Namely, four additional patterns are actively affecting cyclone occurrences in various regions in the North Atlantic and European sector. These are the Eurasian pattern, the Scandinavian pattern, the East Atlantic/West Russian pattern and Polar Eurasian pattern. The details presented in the result section show that the SN cyclone behaviour's link to the larger scales to some extent in agreement with findings in M06 where EW cyclones were investigated. However, as we here distinguished between cyclone tracks with meridional components in either direction, some additional details appeared:

- The areas of NAO influence on NS cyclones over central Canada/North America and on SN cyclones over the northern North Atlantic/Nordic Seas add up the area of NAO influence on WE cyclones (M06 figure 8).
- The EAP has a similar effect on SN cyclones as WE cyclones.
- SCA and EA/WR patterns have opposite effects on SN and NS cyclones. I.e. areas where NS cyclones are favoured in the positive phase in either of these patterns seem to be favourable locations for SN cyclones in the negative phase. Thus it is likely that the aggregated effect of these patterns on the two cyclone classes is similar to their effect on the WE cyclones (which to a large extent contain SN and NS cyclones). This can also explain the lack of similarity with respect to the two patterns separate effect on WE cyclone variability.

- The polar Eurasian pattern's effect on NS cyclones shows some similarity to it's effect on the WE cyclones. The main difference is that is weaker in the NS case.

For SN cyclones there is some resemblance between NCEP and the model with respect to the large scale influence on cyclone count variability. Both the area of influence and sign exhibit some degree of similarity for all the relevant patterns except the East Atlantic and Polar Eurasian patterns. For the NS cyclones, we find very weak or no influence from the large scale patterns. This is not the case in the NCEP data.

The systematic model errors with respect to cyclone occurrence and variability revealed here has several practical consequences. One is that there must be compensating processes in the model to maintain a realistic climatology. In the Northern Hemisphere synoptic eddies provide a substantial part of the poleward heat transport (Hartmann 1994; Oort 1983). As we find the cyclone counts and their monthly variance to be 30-40% less than in NCEP data, we must conclude that individual low pressure systems in the model are more efficient than the real ones in transporting heat polewards. There is also the possibility that a larger part of the heat transport is provided by the quasi-stationary waves in the model. A more detailed study on these issues will be subject to future work in order to confirm these hypotheses.

Interpretation of regional climate changes associated with cyclones (variability) from global scenario simulations containing the model errors mentioned above, will also be problematic and adds uncertainty to the results.

Also, the reason why we find systematically too low cyclone occurrence (variability) has not been investigated here. We can only speculate that it somehow is linked to the baroclinic structures in the model.

Interestingly, we found that relevant large scale modes had no or very weak connection with cyclone count variability in the model. As we found the spatial structure of the RPCs to be in accordance with observationally based ones, it is likely that the lack of correspondence is linked with the time behaviour of these patterns in the model.

A. Rotated Principal Component Analysis

The Rotated Principal Component Analysis (RPCA) is used to calculate the Northern Hemisphere teleconnection indices. Generally, the Empirical Orthogonal Function (EOF)

analysis is proceeded before rotated procedure. The algorithm of EOF is described as follows:
Use of singular value decomposition (svd) to break up the data matrix into 3 matrices:
$Z = U * D * V^t$
where U and V are orthonormal and D is diagonal. Then,
EOFs = V
ECs = U * D
EOFs is principal component, ECs is principal component time series. At times, the EOFs that result from the analysis will be difficult to explain in terms of physical meaning. In this case, it is often beneficial to rotate the principal component (EOFs) we found to one which can be better explained in terms of physical forces. Here a particularly common orthogonal rotation known as varimax is used, Varimax rotation method maximizes the sparseness of each of EOFs modes by means of an orthogonal rotation. As a result of a Varimax rotation, a new set of EOFs modes is produced; each of these new EOFs modes will have a few components with large amplitude and many with small or nearly zero amplitude, thereby putting the basis closer to the actual data and increasing interpretability.

In this paper, we apply the RPCA technique to monthly mean standardized 500-mb height anomalies obtained from the NCEP in the analysis region 20 ℕ-90 ℕ between January 1948 and October 2005. The anomalies are standardized by the 1948-2005 base period monthly means and standard deviations. Season variability is also considered to detrude from the original data field. Only the three months in winter (DJF) are taken account into the all year's time series, then SVD method is used to calculate the Empirical Orthogonal Function (EOF) analysis, we keep the ten leading unrotated EOFs which explain the most variance contribute of the observed standardized height anomaly field, finally, a Varimax rotation is then applied to these ten leading un-rotated modes, yielding the ten leading rotated modes and their time series. These ten dominant teleconnection patterns are referred to as the North Atlantic Oscillation, the Pacific/North American teleconnection pattern, the East Atlantic pattern, the West Pacific pattern, the East Pacific – North Pacific pattern, the East Atlantic/ Western Russia pattern, the Tropical/ Northern Hemisphere pattern, the Polar-Eurasian pattern, the Scandinavia pattern, and the Pacific Transition pattern. The figures which showed in paper are the patterns which have more relation with Atlantic area, the North Atlantic Oscillation, the East Atlantic pattern, East Atlantic/ Western Russia pattern, the Scandinavia pattern and the Polar-Eurasian pattern.

In the figures a through j, the patterns based on both NCEP and model data are shown. Except for the East Atlantic and Polar Eurasian patterns, the spatial structures show some resemblance between corresponding model and reanalysis patterns. It should be noted that the sign is shifted on the Scandinavian and East Atlantic/Western Russian patterns in the model.

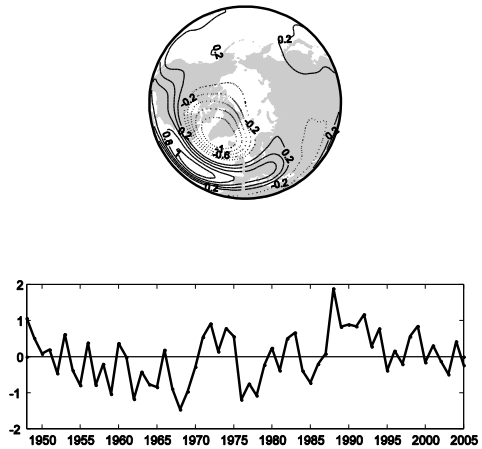

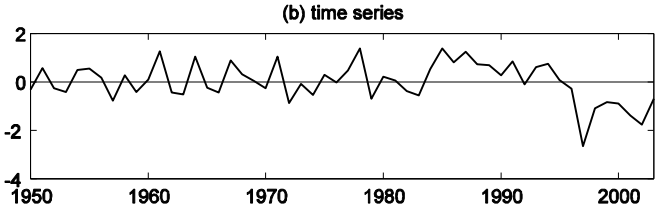

Figure a. The NAO based on NCEP data.

Figure b. The NAO based on ARPEGE simulation

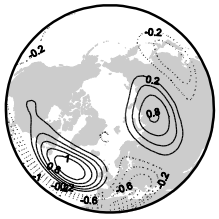

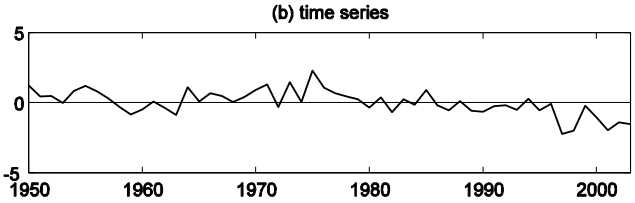

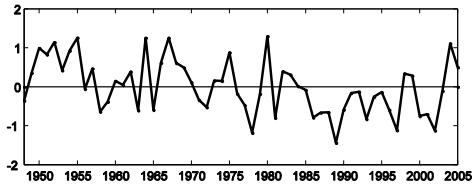

Figure c. East Atlantic Pattern based on NCEP data.

Figure d. East Atlantic Pattern based on simulation

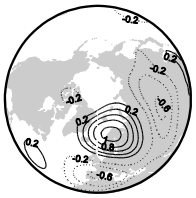

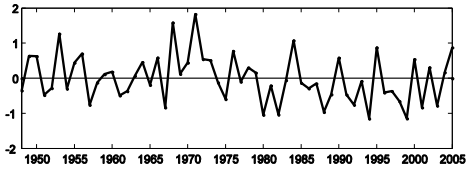

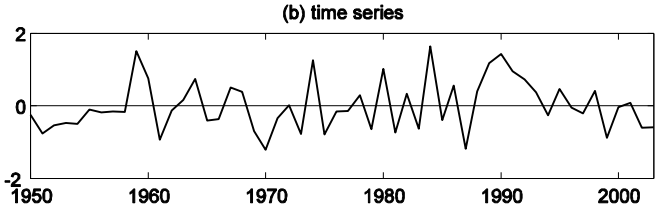

Figure e. Scandinavian pattern based on NCEP.

Figure f. Scandinavian Pattern based on simulation.

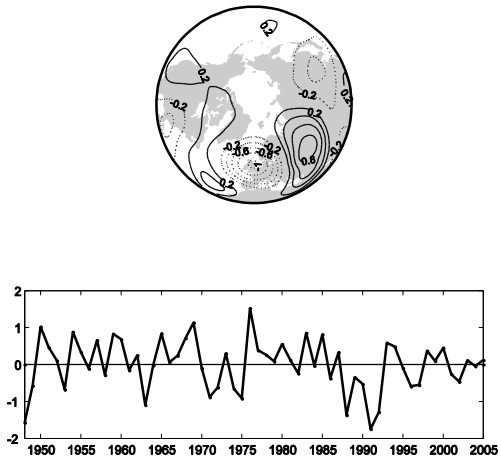

Figure g. The East Atlantic/Western pattern based on NCEP.

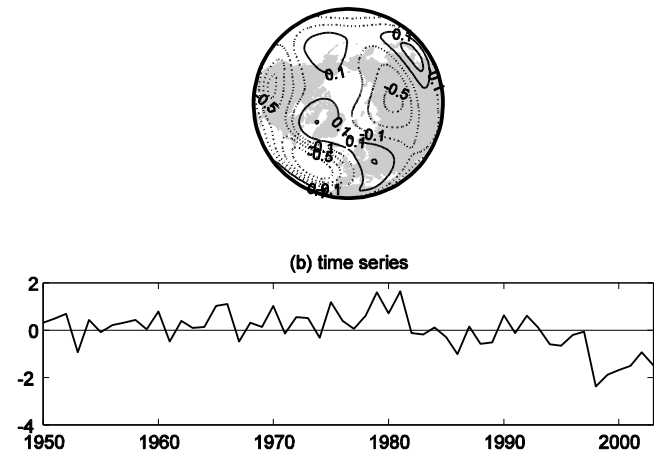

Figure h. The East Atlantic/West Russia pattern based on simulation.

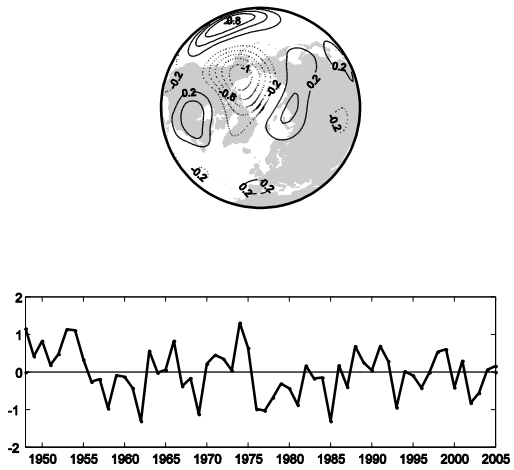

Figure i. The polar Eurasian pattern based on NCEP data.

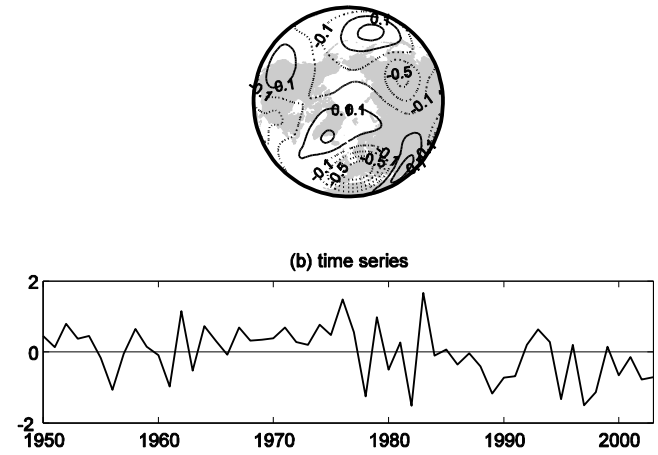

Figure j. The polar Eurasian pattern based on simulation.

References

Akyildiz, V., 1984: Systematic errors in the behaviour of cyclones in the ECMWF operational models. *Tellus*, 37A, 297-308.

Anderson, D., K. I. Hodges, and B. J. Hoskins, 2003: Sensitivity of feature-based analysis methods of storm tracks to the form of background field removal. *Mon. Wea. Rev.*, 131, 565-573.

Barnston, A. G., and R. E. Livezey, 1987: Classification, seasonality and persistence of low-frequency atmospheric circulation patterns. *Mon. Wea. Rev.*, 115, 1083-1126.

Blackmon, M. L., 1976: A climatological spectral study of the 500-mb geopotential height of the Northern Hemisphere. *J. Atmos. Sci.*, 33, 1607–1623.

——,J. M. Wallace, N.-C. Lau and S. L. Mullen, 1977: An observational study of the Northern Hemisphere wintertime circulation. *J. Atmos. Sci.*, 34, 1040–1053.

——,Y. Lee and J. Wallace, 1984: Horizontal structure of 500-mb height fluctuations with long, intermediate, and short time scales. *J. Atmos. Sci.*, 41, 961–979.

Bergeron, T., 1954: The problem of tropical hurricanes. *Q. J. R. Meteor. Soc.*, 80, 131-164.

Bossuet C, Deque M, Cariolle D, 1998 : Impact of a simple parameterization of convective gravity-wave drag in a stratosphere-troposphere general circulation model and its sensitivity to vertical resolution. Annales Geophysicae-Atmospheres Hydrospheres and Space Sciences, 16 (2): 238-249

Cai, M., and H. M. Van den Dool, 1991: Low-frequency waves and traveling storm tracks. Part I: Barotropic component. *J. Atmos. Sci.*, 48, 1420–1444.

Chang, E. K. M. and Y. Fu, 2002: Interdecadal variations in Northern Hemisphere winter storm track intensity. *J. Clim.*, 15, 642-658.

Déqué M., C. Dreveton, A. Braun and D. Cariolle, 1994: The ARPEGE/IFS atmosphere model- a contribution to the French Community Climate Modeling. *Clim. Dyn.*, 10, 249-266.

Déqué M., P. Marquet, and R. G. Jones, 1998: Simulation of climate change over Europe using a global variable resolution general circulation model. *Clim. Dyn.*, 14, 173-189.

Doblas-Reyes F. J., M. Deque, F. Valero, and D. B. Stephenson, 1998: North Atlantic wintertime intraseasonal variability and its sensitivity to GCM horizontal resolution. *Tellus A*, 50, 573-595.

Douville H, Royer JF, Mahfouf JF 1995: A new snow parameterization for the Meteo-France climate model. Part II: Validation in a 3-D GCM experiment, Clim. Dyn. 12 (1): 37-52.

Gibson, J. K., P. Kållberg, S. Uppala, A. Hernandez, A. Nomura and E. Serrano, 1997: ERA description. ECMWF re-analysis project report series, No. 1, ECMWF, Reading, United Kingdom, 71pp.

Harmann, D. 1994: Global Physical Climatology, Vol. 56, International Geophysics Series, London: Academic Press.

Hodges, K. I., 1994: A general method for tracking analysis and its application to meteorological data. *Mon. Wea. Rev.*, 122, 2573-2586.

——, 1995: Feature tracking on the unit sphere. *Mon. Wea. Rev.*, 123, 3458-3465.

——, 1996: Spherical nonparametric estimators applied to the UGAMP model integration for AMIP. *Mon. Wea. Rev.*, 124, 2914-2932.

——, 1999: Adaptive constrains for feature tracking. *Mon. Wea. Rev.*, 127, 1362-1373.

——, B. J. Hoskins, J. Boyle and C. Thorncroft, 2003: A comparison of recent re-analysis datasets using objective feature tracking: storm tracks and tropical easterly waves. *Mon. Wea. Rev.*, 131, 2012-2037.

Hortal, M. 1998: Aspects of the numerics of the ECMWF model. ECMWF seminar proceedings: Recent developments in numerical methods for atmospheric modelling, 7 – 11 September 1998, pp 127 – 143, ECMWF, Shinfield Park, Reading, Berkshire, UK.

Hoskins B. J. and K. I. Hodges, 2002: New perspectives on the Northern Hemisphere winter storm tracks. *J. Atmos. Sci.*, 59, 1041–1061.

Hurrell, J. W. 1995: Decadal trends in the North Atlantic Oscillation: regional temperatures and precipitation. *Science*, 269, 676-679.

Kalnay, E. and coauthors, 1996: The NCEP/NCAR 40-year reanalysis project. *Bull. Amer. Meteorol. Soc.*, 77, 437-471.

Lau, N.-C., 1988: Variability of the observed midlatitude storm tracks in relation to low-frequency changes in the circulation pattern. *J. Atmos. Sci.*, 45, 2718–2743.

Lopez P., T. Schmith, and E. Kaas, 2000: Sensitivity of the Northern Hemisphere circulation to North Atlantic SSTs in the ARPÈGE Climate AGCM. *Clim. Dyn.*, 16, 535-547.

Lott F, Miller M.J, 1997: A new subgrid-scale orographic drag parametrization: Its formulation and testing. *Q.J.R.M.S.* 123 Part A (537): 101-127

Mailier, P.J., D.B. Stephenson, C.A.T. Ferro, and K.I. Hodges, 2006: Serial Clustering of Extratropical Cyclones , *Mon. Wea. Rev.*, 134, 2224-2240.

Morcrette, J.-J., 1991: Radiation and cloud radiative properties in the European Centre for Medium Range Forecasts forecasting sys-tem. *J.Geophys.Res.*, 96, D5, 9121 - 9132.

Murray, R. J. and I. Simmonds, 1991: A numerical scheme for tracking cyclone centres from digital data. Part I: development and operation of the scheme. *Aust. Meteor. Mag.*, 39, 155-166.

Oort, A.H., 1983: Global Atmospheric Circulation Statistics, 1958 – 1973. NOAA, Prof. Pap., 14, U.S. Government Printing Office, Washington DC, 180pp.

Petterssen, S., 1950: Some aspects of the general circulation. *Centennial Proc. Royal Meteorological Society*, Oxford, United Kingdom, *Roy. Meteor. Soc.*, 120-155

Reynolds, R. W. and T. M. Smith, 1994: Improved global sea surface temperature analyses using optimum interpolation. *J. Clim.*, 7, 929-948.

Roger, J. C., 1997: North Atlantic Storm Track Variability and Its association to the North Atlantic Oscillation and Climate Variability of Northern Europe. *J. Clim.*, 10, 1635-1646.

Serreze, M. C., J. E. Box, R. G. Barry and J. E. Walsh, 1993: Charactistics of Arctic synoptic activity, 1952-1989. *Meteor. Atmos. Phy.*, 51, 147-164.

Simmons, A.J. and Burridge, D.M., 1981: An energy and angular momentum conserving vertical finite-difference scheme and hybrid vertical coordinate. *Mon.Wea.Rev.*, 109, 758-766.

Simmons, A. J., and J. K. Gibson, 2000: The ERA-40 project plan. ECMWF ERA-40 Project Report Series 1, ECMWF, Reading, United Kingdom. (Available online at http//www.ecmwf.int/publications/library/do/references/list/192)

Sorteberg, A., N. G. Kvamstø and Ø. Byrkjedal, 2004: Wintertime Nordic Sea cyclone variability and its impact on oceanic volume transports into the Nordic Seas. *The Nordic Seas: An Integrated Perspective*, Geophysical Monograph 158, 137-156.

Thompson, D. W. J. and J. M. Wallace, 2000: Annular modes in the extratropical circulation, Part I: month-to-month variability. *J. Clim.*, 13, 1000-1016.

Thompson, D. W. J., J. M. Wallace and G. C. Hegerl, 2000: Annular modes in the extratropical circulation, Part II: trends. *J. Clim.*, 13, 1018-1036.

Wallace J. M. and D. S. Gutzler, 1981: Teleconnection in the geopotential height field during the Northern Hemisphere winter, *Mon. Wea. Rev.*, 109, 784-812.

Zhang D. and E. Altshuler, 1999: The Effects of Dissipative Heating on Hurricane Intensity. *Mon. Wea. Rev.*, 127, 3032–3038.

Zolina O., and S. K. Gulev, 2002: Improving the accuracy of mapping cyclone numbers and frequencies. *Mon. Wea. Rev.*, 130, 748-759.